Molecular Crystals and Liquid Crystals
Publication details, including instructions for authors and subscription information:
http://www.tandfonline.com/loi/gmcl20

Liquid Crystalline Properties of Unsymmetrical N-(o-hydroxybenzylidene)-N′-(4-n-alkoxybenzoyloxybenzylidene)azines: Synthesis and Characterization

Bachcha Singh [a] & Ashwini Pandey [a]

[a] Department of Chemistry, Faculty of Science, Banaras Hindu University, Varanasi, India

Version of record first published: 01 Mar 2010

To cite this article: Bachcha Singh & Ashwini Pandey (2010): Liquid Crystalline Properties of Unsymmetrical N-(o-hydroxybenzylidene)-N′-(4-n-alkoxybenzoyloxybenzylidene)azines: Synthesis and Characterization, Molecular Crystals and Liquid Crystals, 517:1, 148-158

To link to this article: http://dx.doi.org/10.1080/15421400903483973

Mol. Cryst. Liq. Cryst., Vol. 517: pp. 148–158, 2010
Copyright © Taylor & Francis Group, LLC
ISSN: 1542-1406 print/1563-5287 online
DOI: 10.1080/15421400903483973

Liquid Crystalline Properties of Unsymmetrical *N*-(*o*-hydroxybenzylidene)-*N′*-(4-n-alkoxybenzoyloxybenzylidene)azines: Synthesis and Characterization

BACHCHA SINGH AND ASHWINI PANDEY

Department of Chemistry, Faculty of Science, Banaras Hindu University, Varanasi, India

A new series of mesogenic unsymmetrical azines, N-*(*o*-hydroxybenzylidene)*-N′-*(4-*n-*alkoxybenzoyloxybenzylidene)azines,* $HOC_6H_4CH{=}N\text{-}N{=}CHC_6H_4OCOC_6H_4OC_mH_{2m+1}$ *(m = 7, 8, 9, 10, 11, 12, 14, and 16) have been prepared. They have been characterized by elemental analyses, FT-IR, UV-visible,* ^1H*, and* ^{13}C *NMR (Nuclear Magnetic Resonance) spectra. The mesomorphic properties of these compounds were investigated by differential scanning calorimetry (DSC) and polarized optical microscopy (POM). The azines m = 7, 10, and 14 exhibit features of enantiotropic nematic (N) mesophase whereas azines m = 8, 11 exhibit features of a monotropic nematic phase. The azines m = 9, 12, and 16 do not exhibit mesogenic nature.*

Keywords Differential scanning calorimetry; enantiotropic nematic mesophase; monotropic nematic mesophase; polarized optical microscopy

1. Introduction

Azines (or diimines) have been extensively studied due to their utility in a number of interesting organic reactions and applications [1,2]. Furthermore, they have received attention as possible nonlinear optical (NLO) materials, especially the unsymmetrical azines with an electron donor on one side and an electron acceptor on the other side [3–5]. Azines have been used for the preparation of the nematic liquid crystals and liquid crystal display devices such as TN-LCD (twisted nematic-LCD), STN-LCD (supertwisted nematic-LCD) and TFT-LCD (thin film transistor-LCD) having improved electro-optical properties [6,7]. Wilfrid and Glenn [8] reported a series of azine liquid crystals having high clearing points. Since then experimental and theoretical studies [9–15] have been carried out on the synthesis and mesomorphic properties of azine type liquid crystals.

Yang et al. [16] reported two series of new symmetrical azine based liquid crystals, 4,4′-(4-alkylbenzoyloxy)-benzalazine that contain only ester groups in their

---

Address correspondence to Bachcha Singh, Department of Chemistry, Faculty of Science, BHU, Varanasi-221005, India. E-mail: bsinghbhu@rediffmail.com

linear mesogenic core and alkyl or alkoxy end groups. The end groups of the liquid crystals had an effect on their mesomorphic properties. The series with alkoxy end groups exhibited both smectic A and nematic mesophase whereas the series with alkyl end groups showed only nematic phase at their lower analogues and showed both smectic A and nematic properties at their higher analogues.

Chudgar et al. [15] reported a series of azine type liquid crystals with ester group and lateral substituents in the rigid core and alkoxy end groups. Kelker and coworkers [17] reported Schiff base liquid crystals 4-methoxybenzylidene-4′-butylaniline (MBBA) which exhibits a room temperature nematic phase. Since then, Schiff bases based on esters have attracted much attention on liquid crystal researches. Over the past few decades, a lot of low molar mass Schiff base esters have been synthesized and investigated extensively for liquid crystalline applications [18–23]. Centore and Garzillo [24] reported a structural and theoretical analysis of biphenylene azines containing a methyl group on the azine system and strong electron donor-acceptor groups on the phenylene rings. Centore et al. [5] reported asymmetrical azines which show both nematic and smectic phases.

The literature survey reveals that a few reports are available on synthesis, characterization, and mesomorphic properties of ester based unsymmetrical azines.

The synthesis, characterization, and mesomorphic properties of hitherto uninvestigated new series of ester based unsymmetrical azines liquid crystals *N*-(*o*-hydroxybenzylidene)-*N*′-(4-n-alkoxybenzoyloxybenzylidene)azines (**6**) have been under taken. The results of these investigations are reported in this article.

2. Experimental

2.1. *Materials*

Salicylaldehyde (Spectrochem), hydrazine monohydrate (Qualigens), pyridine (Qualigens), thionyl chloride (Qualigens), 4-hydroxybenzaldehyde (AcrosOrganic), 4-hydroxybenzoic acid (Aldrich), and 1-bromoalkanes (Aldrich) were used as received. All other solvents and reagents were purchased commercially and used after further purification.

2.2. *Techniques*

Elemental analyses were performed on CE-440 Exeter Analytical CHN analyzer. Infrared (IR) spectra (4000–100 cm^{-1}) were recorded on Varian 3100 FT-IR Excalibur spectrophotometer. ^{1}H and ^{13}C NMR spectra were obtained by using a JEOL FT NMR AL 300 MHz spectrometer using tetramethylsilane as internal standard. Electronic spectra were recorded on UV-1700 Pharma Spec Shimadzu UV-Visible spectrophotometer. Differential scanning calorimetry (DSC) thermograms were recorded on Mettler Toledo TC 15 TA differential scanning calorimeter at the rate of 10.0 Kmin^{-1} under nitrogen atmosphere using spec pure grade indium as standard by taking samples in close lid aluminum pans. The transition temperatures from DSC have been determined with accuracy of ±0.1 K. The mesophase type was assigned by visual comparison with known phase standards using HT-30.01 NTT 268 LOMO polarizing optical microscope fitted with a hot stage with temperature controlling accuracy of 0.1 K.

2.3. *Synthesis of Compounds*

2.3.1. *Synthesis of Salicylhydrazone **4***. Salicylhydrazone was synthesized by the procedure as mentioned elsewhere [25].

2.3.2. *Synthesis of 4-(4′-heptyloxybenzoyloxy)benzaldehyde **5***. 4-Heptyloxybenzoic acid (1.41 g, 6 mmol) was dissolved in dry chloroform (55 ml) and thionyl chloride (0.51 ml, 7 mmol) was added and refluxed for 8 h. The solvent was removed under reduced pressure to give a yellow oil. It was further treated with a solution of 4-hydroxybenzaldehyde (0.73 g, 6 mmol) in dry chloroform (50 ml) in the presence of 2–3 drops of pyridine. The mixture was then refluxed for 9 h. After cooling, light yellow solution was washed with water (50 ml), dried over anhydrous $MgSO_4$, and then concentrated to form white crystals of 4-(4′-heptyloxybenzoyloxy) benzaldehyde. Yield: 72%. IR (KBr, cm^{-1}): 2924, 2854 (aliphatic C−H), 1776 (C=O ester), 1712 (C=O aldehyde), 1605, 1511 (Ph), 1307, 1258 (OPh). ^1H NMR 300 MHz ($CDCl_3$, TMS) δ_H (ppm): 10.02 (s, 1 H, CHO), 8.15–6.88 (m, 8 H, ArH), 4.07–3.97 (m, 2 H, $-OCH_2$), 1.81–1.27 (m, 10 H, $-[CH_2]_n$), 0.90–0.86 (t, 3 H, $-CH_3$).

All other homologous members of the series were prepared following the above procedure.

2.3.3. *Synthesis of Unsymmetrical* N-*(*o*-hydroxybenzylidene)*-N′-*(4-n-heptyloxybenzoyloxybenzylidene)azine **6a***. A mixture of salicylhydrazone (0.13 g, 6 mmol) and 4-(4′-heptyloxy benzoyloxy)benzaldehyde (2.38 g, 6 mmol) in 45 ml of chloroform containing 3–4 drops of glacial acetic acid was stirred for 7 h. A yellow solution was obtained which was evaporated under reduced pressure to yield cream colour crystals. The product was washed with water and recrystallized from methanol. All other homologous members of the series were prepared in a similar manner. Their IR, analytical, NMR data are summarized as follows.

2.3.4. N-*(*o*-hydroxybenzylidene)*-N′-*(4-n-heptyloxybenzoyloxybenzylidene)azine, $C_{28}H_{30}N_2O_4$ (**6a**)*. Yield: 65%. IR (KBr, cm^{-1}): 3445 (OH), 2925, 2854 (aliphatic C−H), 1727 (C=O ester), 1681 (C=N), 1613 (Ph), 1259 (OPh), 1018 (N−N). ^1H NMR 300 MHz ($CDCl_3$, TMS) δ (ppm): 11.37 (s, 1 H, −OH), 8.71 (s, 1 H, $-C_6H_4OHC\underline{H}=N$), 8.67 (s, 1 H, $ROC_6H_4C\underline{H}=N$), 8.15–6.90 (m, 12 H, ArH), 4.04–3.99 (t, $\underline{2}$ H, $-OCH_2$), 1.85–1.32 (m, $\overline{10}$ H, $-[CH_2]_n$), 0.90–0.89 (t, 3 H, $-CH_3$). ^{13}C NMR δ_c ($CDCl_3$): 164.6 (COO ester), 163.6 (CH=N), 161.8, 159.7 (C−OH), 153.3, 133.4, 132.5 (Ar−C), 132.3, 131.5, 129.7, 122.2, 121.5, 119.7, 117.2, 117.1, 114.3, 114.1, 77.4, 77.0, 76.5 ($CDCl_3$, 3 peaks), 68.3 ($-OCH_2$), 68.2, 31.7, 29.0, 25.9 ($OCH_2\underline{C}H_2$), 22.5, 14.0 (CH_3). UV-visible ($CHCl_3$): $\lambda_{max} = 451$, 376, 304, 269 nm. Elemental analyses: calculated (for $C_{28}H_{30}N_2O_4$), C, 73.34; H, 6.59; N, 6.10%, found, C, 73.02; H, 6.34; N, 6.02%.

2.3.5. N-*(*o*-hydroxbenzylidene)*-N′-*(4-n-octyloxybenzoyloxybenzylidene)azine, $C_{29}H_{32}N_2O_4$ (**6b**)*. Yield: 60%. IR (KBr, cm^{-1}): 3446 (OH), 2927, 2857 (aliphatic C−H), 1728 (C−O ester), 1682 (C=N), 1616 (Ph), 1263 (OPh), 1017 (N−N). ^1H NMR 300 MHz ($CDCl_3$, TMS) δ (ppm): 11.37 (s, 1 H, −OH), 8.71 (s, 1 H, $-C_6H_4OHC\underline{H}=N$), 8.67 (s, 1 H, $ROC_6H_4C\underline{H}=N$), 8.15–6.90 (m, 12 H, ArH), 4.04–3.99 (t, $\underline{2}$ H, $-OCH_2$), 1.82–1.29 (m, $12\,\overline{H}$, $-[CH_2]_n$), 0.89 (t, 3 H, $-CH_3$). ^{13}C NMR δ_C ($CDC1_3$): 164.6 (COO ester), 163.6 (CH=N), 161.1, 159.7 (C−OH), 153.3, 133.4, 132.5 (Ar−C), 132.3, 132.2, 131.4, 129.7, 122.2, 121.1, 119.7, 117.2, 117.1, 114.3, 114.1, 113.9, 77.4, 77.0, 76.5 ($CDC1_3$, 3 peaks), 68.3 ($-OCH_2$), 68.2, 31.7, 29.3, 29.1, 29.0, 25.9 ($OCH_2\underline{C}H_2$), 22.6, 14.0 (CH_3). UV-visible ($CHC1_3$): $\lambda_{max} = 446$, 307, 269 nm. Elemental analyses: calculated (for $C_{29}H_{32}N_2O_4$), C, 73.70; H, 6.82; N, 5.92%, found, C, 73.82; H, 6.56; N, 5.83%.

2.3.6. N-*(o-hydroxybenzylidene)*-N′-*(4-n-nonyloxybenzoyloxybenzylidene)azine,* $C_{30}H_{34}N_2O_4$ ***(6c).*** Yield: 62%. IR (KBr, cm^{-1}): 3449 (OH), 2919, 2851 (aliphatic C−H), 1736 (C=O ester), 1680 (C=N), 1606 (Ph), 1263 (OPh), 1017 (N−N). ^1H NMR 300 MHz ($CDC1_3$, TMS) δ (ppm): 11.37 (s, 1 H, −OH), 8.71 (s, 1 H, $-C_6H_4OHC\underline{H}{=}N$) 8.67 (s, 1 H, $ROC_6H_4C\underline{H}{=}N$), 8.15–6.90 (m, 12 H, ArH), 4.04–3.99 (t, $\underline{2}$ H, $-OCH_2$), 1.82–1.29 (m, $\underline{14}$ H, $-[CH_2]_n$), 0.89 (t, 3 H, $-CH_3$). ^{13}C NMR δ_C ($CDC1_3$): 164.6 (COO ester), 163.6 (CH=N), 161.1, 159.7 (C−OH), 153.3, 133.4, 132.5 (Ar−C), 132.3, 132.2, 131.4, 129.7, 122.2, 121.1, 119.7, 117.2, 117.1, 114.3, 114.1, 113.9, 77.4, 77.0, 76.5 ($CDC1_3$, 3 peaks), 68.3 ($-OCH_2$), 68.2, 31.7, 29.3, 29.1, 29.0, 25.9 ($OCH_2\underline{C}H_2$), 22.6, 14.0 (CH_3). UV-visible ($CHC1_3$): $\lambda_{max} = 444$, 373, 309, 268 nm. Elemental analyses: calculated (for $C_{30}H_{34}N_2O_4$), C, 74.04; H, 7.04; N, 5.75%, found, C, 74.12; H, 7.13; N, 5.36%.

2.3.7. N-*(o-hydroxybenzylidene)*-N′-*(4-n-decyloxybenzoyloxybenzylidene)azine,* $C_{31}H_{36}N_2O_4$ ***(6d).*** Yield: 59%. IR (KBr, cm^{-1}): 3445 (OH), 2923, 2854 (aliphatic C−H), 1728 (C = O ester), 1680 (C=N), 1614 (Ph), 1261 (OPh), 1019 (N−N). ^1H NMR 300 MHz ($CDC1_3$, TMS) δ_H (ppm): 11.37 (s, 1 H, −OH), 8.71 (s, 1 H, $-C_6H_4OHC\underline{H}{=}N$), 8.67 (s, 1 H, $ROC_6H_4C\underline{H}{=}N$), 8.15–6.96 (m, 12 H, ArH), 4.07–4.02 (t, $\underline{2}$ H, $-OCH_2$), 1.84–1.28 (m, $\underline{16}$ H, $-[CH_2]_n$), 0.88 (t, 3 H, $-CH_3$). UV-visible ($CHC1_3$): $\lambda_{max} = 347$, 305, 273, 263 nm. Elemental analyses: calculated (for $C_{31}H_{36}N_2O_4$), C, 74.37; H, 7.24; N, 5.59%, found, C, 74.02; H, 6.92; N, 5.12%.

2.3.8. N-*(o-hydroxybenzylidene)*-N′*(4-n-undecyloxybenzoyloxybenzylidene)azine,* $C_{32}H_{38}N_{24}O_4$ ***(6e).*** Yield: 70%. IR (KBr, cm^{-1}): 3354 (OH), 2922, 2853 (aliphatic C−H), 1727 (C=O ester), 1678 (C=N), 1605 (Ph), 1260 (OPh), 1019 (N−N). ^1H NMR 300 MHz ($CDC1_3$, TMS) δ_H (ppm): 11.39 (s, 1 H, −OH), 8.71 (s, 1 H, $-C_6H_4OHC\underline{H}{=}N$), 8.67 (s, 1 H, $ROC_6H_4C\underline{H}{=}N$), 8.15–6.90 (m, 12 H, ArH), 4.04–4.00 (t, $\underline{2}$ H, $-OCH_2$), 1.83–1.27 (m, $\underline{18}$ H, $-[CH_2]_n$), 0.89 (t, 3 H, $-CH_3$). UV-visible ($CHCl_3$): $\lambda_{max} = 451$, 379, 270 nm. Elemental analyses: calculated (for $C_{32}H_{38}N_2O_4$), C, 74.68; H, 7.44; N, 5.44%, found, C, 74.52; H, 7.32; N, 5.21%.

2.3.9. N-*(o-hydroxybenzylidene)*-N′-*(4-n-dodecyloxybenzoyloxybenzylidene)azine,* $C_{33}H_{40}N_2O_4$ ***(6f).*** Yield: 66%. IR (KBr, cm^{-1}): 3451 (OH), 2921, 2852 (aliphatic C−H), 1727 (C=O, ester), 1679 (C=N), 1615 (Ph), 1261 (OPh), 1021 (N−N). ^1H NMR 300 MHz ($CDC1_3$, TMS) δ_H (ppm): 11.37 (s, 1 H, −OH), 8.71 (s, 1 H, $-C_6H_4OHC\underline{H}{=}N$), 8.67 (s, 1 H, $ROC_6H_4C\underline{H}{=}N$), 8.15–6.90 (m, 12 H, ArH), 4.04–3.99 (t, $\underline{2}$ H, $-OCH_2$), 1.82–1.29 (m, $\underline{20}$ H, $-[CH_2]_n$), 0.89 (t, 3 H, $-CH_3$). ^{13}C NMR δ_C ($CDC1_3$): 164.6 (COO), 163.6 (CH=N), 161.8, 159.7 (C−OH), 153.2, 133.2, 132.1 (Ar−C), 132.3, 131.4, 129.6, 122.2, 121.5, 119.7, 117.2, 117.1, 114.3, 114.1, 77.4, 77.0, 76.5 ($CDC1_3$, 3 peaks), 68.3 ($-OCH_2$), 68.2, 31.7, 29.0, 25.9 ($-OCH_2\underline{C}H_2$), 22.5, 14.0 (CH_3). UV-visible ($CHC1_3$): $\lambda_{max} = 331$, 304 nm. Elemental analyses: calculated (for $C_{33}H_{40}N_2O_4$), C, 74.97; H, 7.62; N, 5.29%, found, C, 74.59; H, 7.81; N, 5.01%.

2.3.10. N-*(o-hydroxybenzylidene)*-N′-*(4-n-tetradecyloxybenzoyloxybenzylidene)azine,* $C_{35}H_{44}N_2O_4$ ***(6g).*** Yield: 64%. IR (KBr, cm^{-1}): 3428 (OH), 2923, 2856 (aliphatic C−H), 1726 (C = O ester), 1682 (C=N), 1610 (Ph), 1270 (OPh), 1011 (N−N). ^1H

NMR 300 MHz ($CDCl_3$, TMS) δ_H (ppm): 11.39 (s, 1 H, −OH), 8.71 (s, 1H, $-C_6H_4OHC\underline{H}=N$) 8.67 (s, 1 H, $ROC_6H_4C\underline{H}=N$), 8.15–6.90 (m, 12 H, ArH), 4.04–3.99 (t, $\overline{2}$ H, $-OCH_2$), 1.82–1.29 (m, 24 $\overline{\mathrm{H}}$, $-[CH_2]_n$), 0.89 (t, 3 H, $-CH_3$). UV-visible ($CHCl_3$): $\lambda_{max} = 439$, 314, 270 nm. Elemental analyses: calculated (for $C_{35}H_{44}N_2O_4$), C, 75.50; H, 7.96; N, 5.03%, found, C, 75.91; H, 7.91; N, 5.24%.

2.3.11. N-*(*o*-hydroxybenzylidene)*-N′-*(4-n-hexadecyloxybenzoyloxybenzylidene)azine, $C_{37}H_{48}N_2O_4$ (***6h***).* Yield: 61%. IR (KBr, cm^{-1}): 3446 (OH), 2920, 2851 (aliphatic C−H), 1729 (C=O, ester), 1680 (C=N), 1615 (Ph), 1261 (OPh), 1027 (N−N). ^1H NMR 300 MHz ($CDCl_3$, TMS) δ (ppm): 11.38 (s, 1 H, −OH), 8.71 (s, 1 H, $-C_6H_4OHC\underline{H}=N$) 8.67 (s, 1 H, $ROC_6H_4C\underline{H}=N$), 8.15–6.90 (m, 12 H, ArH), 4.04–3.99 (t, $\overline{2}$ H, $-OCH_2$), 1.80–1.26 (m, 28 $\overline{\mathrm{H}}$, $-[CH_2]_n$), 0.87 (t, 3 H, $-CH_3$). UV-visible ($CHCl_3$): $\lambda_{max} = 445$, 307, 271 nm. Elemental analyses: calculated (for $C_{37}H_{48}N_2O_4$), C, 75.99; H, 8.27; N, 4.79%, found, C, 75.82; H, 8.50; N, 4.50%.

3. Results and Discussion

The compounds *N*-(*o*-hydroxybenzylidene)-*N*′-(4-n-alkoxybenzoyloxybenzylidene)-azines **6a–h** have been prepared as shown in Scheme 1. The elemental data are in agreement with the stoichiometry of the compound. The IR and NMR spectral data are fully consistent with the structure. In the IR spectrum of salicylhydrazone the bands appearing at 3481, 3383, 3288, 1617, 1576, and 1028 cm^{-1} are attributed to v(OH), $v_{as}(NH_2)$, $v_s(NH_2)$, v(Ph), and (N−N) modes, respectively. The IR spectrum of 4-(4′-heptyloxybenzoyloxy)benzaldehyde show absorption bands at 2924, 2854, 1776, 1712, 1605, 1511, 1307, 1258 cm^{-1} assigned to v (aliphatic C−H stretch) v(C=O of phenyl ester), v(C=O of aldehyde), v(Ph), and v(OPh), respectively. The IR spectrum of *N*-(*o*-hydroxybenzylidene)-*N*′-(4-n-heptyloxybenzoyloxybenzylidene)-azine **6a** shows absorption bands at 3445, 2925, 2854, 1727, 1681, 1613, 1259, 1018 cm^{-1} which are assigned to v(OH), v(aliphatic C−H), v(C=O) of phenyl ester, v(C=N), v(Ph), v(OPh), and v(N−N) modes, respectively. The disappearance of the band 1712 cm^{-1} due to v(CH=O) and appearance of a new band at 1681 cm^{-1} due to v(C=N) indicates condensation of aldehyde with amine forming Schiff base. The proton NMR of salicylhydrazone depicts peaks at δ 11.03 (s), 7.87 (s), 7.25–6.83 (m), 5.42 (s) ppm which are attributed to −OH, (CH=N), ring, and NH_2. The proton NMR of 4-(4′-heptyloxybenzoyloxy)benzaldehyde exhibit peaks δ 10.02 (s), 8.15–6.88 (m), 4.07–3.97 (m), 1.81–1.27 (m), and 0.90–0.86 (t) ppm which are assigned to −OH, ring, $-OCH_2$, $-[CH_2]_n$, and $-CH_3$ protons, respectively. The proton NMR spectrum of *N*-(*o*-hydroxybenzylidene)-*N*′-(4-n-heptyloxybenzoyloxybenzylidene)azine **6a** exhibits peaks at δ 11.37 (s, 1 H, −OH), 8.71 (s, 1 H, $-C_6H_4OHC\underline{H}=N$), 8.67 (s, 1 H, $ROC_6H_4C\underline{H}=N$), 8.15–6.90 (m, 12 H, ring), 4.04–3.99 (t, $\overline{2}$ H, $-OCH_2$), 1.85–1.32 (m, 10 $\overline{\mathrm{H}}$, $-[CH_2]_n$), and 0.90–0.89 (t, 3 H, CH_3) ppm, respectively. The signals due to Schiff base formation is observed at 8.71 and 8.67 ppm which correspond to *o*-hydroxy benzylidene and p-alkoxybenzylidene groups, respectively. The signals of three rings overlap and are observed at δ 8.15–6.90. The length of alkyl chain has no significant effect on the position of the signals due to −OH, −CH=N, ring, $-OCH_2$, $-[CH_2]_n$, and $-CH_3$ protons, respectively. The UV-visible spectrum of *N*-(*o*-hydroxybenzylidene)-*N*′-(4-n-heptyloxybenzoyloxybenzylidene)azine **6a** shows bands at 451, 376, 304, 269 nm which are assigned as the transitions due to $n \rightarrow \pi^*$ and $\pi \rightarrow \pi^*$ transitions of the ligand moiety.

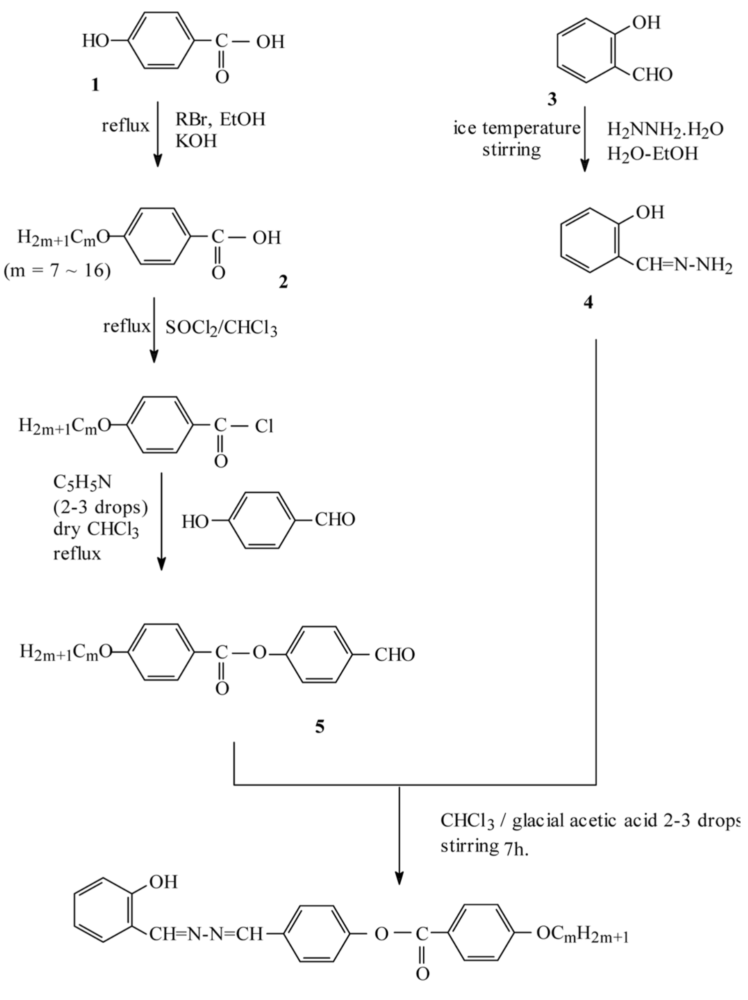

Scheme 1. Synthetic route for *N*-(*o*-hydroxybenzylidene)-*N*′-(4-n-alkoxy benzoyloxybenzylidene)azines.

4. Optical Properties

The liquid crystalline character of *N*-(*o*-hydroxybenzylidene)-*N*′-(4-n-alkoxybenzoyloxybenzylidene)azines **6a–h** were investigated by polarizing optical microscope (POM) observation using a heating and cooling stage. The phase transition temperatures and enthalpies were measured by carrying out DSC thermal analysis. The phase transition temperatures along with the corresponding enthalpy values for the compounds are summarized in Table 1. The symbol K, N, and I are used to denote crystalline, nematic, and isotropic phases, respectively. The compound *N*-(*o*-hydroxybenzylidene)-*N*′-(4-n-heptyloxybenzoyloxybenzylidene)azine **6a** exhibits endothermic peaks at 72.6°C ($\Delta H = 22.28\,\mathrm{kJmol^{-1}}$), 104.6°C ($\Delta H = 0.07\,\mathrm{kJmol^{-1}}$), 145.4°C ($\Delta H = 0.07\,\mathrm{kJmol^{-1}}$), 160.5°C ($\Delta H = 3.27\,\mathrm{kJmol^{-1}}$) due to crystal to crystal transitions while the fourth peak refers crystal to mesophase transition

Table 1. Transition temperatures, transition enthalpy (ΔH), and transition entropy (ΔS) of *N*-(*o*-hydroxybenzylidene)-*N′*-(4-n-alkoxy benzoyloxybenzylidene)azines

Compound	Transitions	T/°C	ΔH/kJmol^{-1}	ΔS/JK^{-1}mol^{-1}
6a	K^1–K^2	72.6	22.28	64.46
	K^2–K^3	104.6	0.07	0.18
	K^3–K^4	145.4	0.07	0.16
	K^4–N	160.5	3.27	7.54
	N–I	192.0	0.05	0.10
	I–N	150.7	0.12	0.28
	N–K^4	109.7	0.13	0.33
	K^4–K	101.2	15.73	42.03
6b	K^1–K^2	49.2	4.40	13.65
	K^2–K^3	72.0	7.18	20.81
	K^3–K^4	85.5	4.88	13.61
	K^4–K^5	111.1	1.47	3.82
	K^5–I	121.1	2.34	5.93
	I–N	109.6	0.07	0.18
	N–K^5	81.9	12.95	36.48
	K^5–K	59.8	6.24	18.75
6c	K^1–K^2	64.6	0.09	0.26
	K^2–I	220.0	25.20	51.11
	I–K	93.7	0.11	0.30
6d	K^1–K^2	41.6	1.69	5.37
	K^2–K^3	53.6	0.04	0.12
	K^3–K^4	56.6	0.06	0.18
	K^4–K^5	64.4	0.06	0.17
	K^5–K^6	69.8	0.23	0.67
	K^6–K^7	80.8	1.32	3.73
	K^7–K^8	104.4	0.05	0.13
	K^8–K^9	119.7	6.72	17.11
	K^9–N	139.9	1.73	4.18
	N–I	183.6	0.20	0.43
	I–N	109.6	0.10	0.26
	N–K^9	95.8	10.39	28.17
	K^9–K	62.1	2.79	8.32
6e	K^1–K^2	48.4	14.61	45.45
	K^2–K^3	71.8	2.05	5.94
	K^3–K^4	90.9	4.99	13.71
	K^4–K^5	104.9	0.81	2.14
	K^5–K^6	145.9	0.26	0.62
	K^6– K^7	187.1	0.23	0.49
	K^7–I	191.9	0.45	0.96
	I–N	150.5	0.59	1.39
	N–K^7	109.5	0.83	2.16
	K^7– K	71.6	19.41	56.32
6f	K^1–K^2	64.5	0.92	2.72
	K^2–K^3	92.4	13.43	36.75

(*Continued*)

Table 1. Continued

Compound	Transitions	T/°C	ΔH/kJmol^{-1}	ΔS/JK^{-1}mol^{-1}
	K^3–K^4	104.6	0.05	0.13
	K^4–K^5	111.3	1.64	4.26
	K^5–K^6	164.4	7.55	17.26
	K^6–K^7	187.1	0.07	0.15
	K^7–I	192.0	0.15	0.32
	I–K^7	150.0	0.27	0.63
	K^7–K^6	109.4	0.39	1.01
	K^6–K^5	98.1	17.76	47.85
	K^5–K^4	83.9	0.13	0.36
	K^4–K	51.8	14.92	45.93
6g	K^1–K^2	64.5	0.06	0.17
	K^2–K^3	78.2	23.85	67.91
	K^3–N	104.6	2.60	6.88
	N–I	192.0	0.03	0.06
	I–N	150.6	0.08	0.18
	N–K^3	109.5	0.13	0.33
	K^3–K	87.3	0.03	0.08
6h	K^1–K^2	77.8	16.29	46.43
	K^2–K^3	90.9	1.80	4.94
	K^3–K^4	121.9	4.64	11.74
	K^4–K^5	170.4	9.20	20.74
	K^5–I	192.0	0.12	0.25
	I–K^5	150.7	0.20	0.47
	K^5–K^4	109.7	0.35	0.91
	K^4–K^3	98.6	18.71	50.34
	K^3–K	62.5	2.71	8.07

and the one observed at 192.0°C is assigned as mesophase to isotropic liquid transition. The exothermic peaks were observed at 150.7°C ($\Delta H = 0.12\,kJmol^{-1}$) and 109.7°C ($\Delta H = 0.13\,kJmol^{-1}$) and 101.2°C ($\Delta H = 15.73\,kJmol^{-1}$) which corresponds to isotropic to mesophase and mesophase to crystal followed by the next crystal phase. The texture of the mesophase observed under polarizing microscope is characteristic of enantiotropic nematic mesophase appearing in both heating and cooling cycle. The nematic droplets that are formed during transition from isotropic phase to nematic mesophase exhibits a characteristic texture depending on the droplet size and the director orientation at the isotropic nematic interface. The texture for the flat compound **6a** between crossed polarizer resulting from surface orientation of the director of the boundaries of the sample and by defects formed in the sample shows a network of black brushes connecting center of points and line defects giving rise to disclination lines which are defect in molecular orientational order. These disclination lines are producing a schlieren optical texture in nearly vertical orientation whose projection are seen as dark points with 2–4 emerging dark stripes or brushes. These black brushes are located in region where the director lies in the plane of polarization of the polarizer or analyzer. Similar phase transitions and enantiotropic nematic mesophase in both heating and cooling cycle showing similar textural patterns are observed for the compounds **6d** and **6g**, respectively. The compound *N*-(*o*-hydroxybenzylidene)-*N*′-(4-n-octyloxybenzoyloxybenzylidene)azine **6b** exhibits sharp endothermic peaks at 49.2°C ($\Delta H = 4.40\,kJmol^{-1}$), 72.0°C ($\Delta H = 7.18\,kJmol^{-1}$), 85.5°C ($\Delta H = 4.88\,kJmol^{-1}$), 111.1°C ($\Delta H = 1.47\,kJmol^{-1}$) corresponding to subsequent crystal to crystal phase transitions (i.e., polymorphism) and the one at 121.1°C exhibit crystal to isotropic liquid phase transition. The exothermic peaks at 109.6°C ($\Delta H = 0.07\,kJmol^{-1}$), 81.9°C ($\Delta H = 12.95\,kJmol^{-1}$), and 59.8°C ($\Delta H = 6.24\,kJmol^{-1}$) show isotropic to mesophase and mesophase to crystal phase transitions which on the basis of optical microscope displays monotropic nematic mesophase with schlieren texture with planar alignment showing defect centers with 2–4 emerging brushes. This compound under crossed polarizer shows a nucleus which is the center of a points or line defect from which black brushes originate. A nucleus can indicate either the disclination line terminating at the surface of a sample or an isolated defect. Similar phase transitions and monotropic nematic phase with schlieren texture are seen for compound **6e**.

The compound **6f** exhibits endothermic peaks at 64.5°C ($\Delta H = 0.92\,kJmol^{-1}$), 92.4°C ($\Delta H = 13.43\,k\,Jmol^{-1}$), 104.6°C ($\Delta H = 0.05\,kJmol^{-1}$), 111.3°C ($\Delta H = 1.64\,kJmol^{-1}$), 164.4°C ($\Delta H = 7.55\,kJmol^{-1}$), 187.1°C ($\Delta H = 0.07\,kJmol^{-1}$), corresponding to subsequent crystal to crystal phase transitions and the one at 192.0°C is assigned to crystal to isotropic phase transition. The exothermic peaks for this compound are exhibited at 150.0°C ($\Delta H = 0.27\,kJmol^{-1}$), 109.4°C ($\Delta H = 0.39\,kJmol^{-1}$), 98.1°C ($\Delta H = 17.76\,kJmol^{-1}$), 83.9°C ($\Delta H = 0.13\,kJmol^{-1}$), and 51.8°C ($\Delta H = 14.92\,kJmol^{-1}$), respectively, which are assigned as isotropic to crystal followed by subsequent crystal to crystal phase transition with no existence of mesophase in both the cycles. This compound exhibits polymorphic behavior (crystal to crystal phase transition) in both the cycle, and no mesophase was thus identified on the basis of DSC measurements and optical microscopy. Similar phenomenon of polymorphism showing subsequent crystal to crystal phase transition both in heating and cooling cycle along with similar optical behavior was recorded for compound **6h**. The compound *N*-(*o*-hydroxybenzylidene)-*N*′-(4-n-nonyloxybenzoyloxybenzylidene)azine **6c** exhibited two endothermic peaks at 64.6°C ($\Delta H = 0.09\,kJmol^{-1}$) and 220°C pertaining to crystal to crystal phase transition and crystal to isotropic phase respectively followed by single exothermic peaks at 93.7°C ($\Delta H = 0.11\,kJmol^{-1}$) which defines a sudden phase transition from isotropic to crystal phase. However, the compound failed to show optical texture as viewed under cross polaroids. The thermotropic nematic mesophase pattern based on the structural correlation of these compounds reveals a calamitic geometry for all the homologues of the series. The presence of ester linker moiety between the two phenyl groups plays a major role for the emergence of nematic mesophase in these series of compounds. It is known that the presence of ester bridging group increases flexibility and mobility of particular parts of liquid crystal molecule and hence affects the type of mesophase and its temperature range [26]. The study based on unsymmetrical azines with ether bridging moiety has revealed to the emergence of nematic and smectic A mesophases [27]. The substitution of ether linkage with the ester moiety along with the incorporation of aromatic ring with long alkoxy chain results in suppression of smectic A mesophase and leads to the occurrence of nematic phase in some homologs of the series. Thus, it may be concluded that by the replacement of –OR with –OOC–C_6H_4–OR, the orderness of the system decreases.

5. Conclusions

A new series of unsymmetrical N-(*o*-hydroxybenzylidene)-N′-(4-n-alkoxy benzoyloxybenzylidene)azines have been synthesized having terminal alkoxy chains (m = 7–16). The chemical structures of the final products were investigated by FT-IR, NMR, UV-visible, ^{1}H, and ^{13}C NMR spectra. The mesomorphic properties and optical textures of the products were characterized by DSC and POM. The existence of nematic mesophase (schlieren texture) was confirmed by POM. It was found that the bridging ester moiety between the aromatic rings with long alkoxy chain leads to the occurrence of nematic phase as the replacement of –OR by –OOC–C_6H_4–OR decreases the ordernes of the system.

Acknowledgement

The authors thank the Head, Department of Chemistry, BHU, Varanasi for providing laboratory facilities. One of the authors (AP) thanks BHU for research scholarship. Thanks are also due to Mr. Satish Tiwari for CHN and DSC analyses, Mr. R. C. P. Bipin for NMR and Mr. V. N. Pandey for IR and electronic spectral data. We are grateful to Dr. R. Dhar, Ewing Christian College, Allahabad for suggestions regarding the texture analysis.

References

[1] Giroud-Godguin, A. M., & Maitlis, P. M. (1991). *Angew. Chem., Int. Ed.*, *30*, 375.
[2] Hudson, S. A., & Maitlis, P. M. (1993). *Chem. Rev.*, *93*, 861.
[3] Nalwa, H. S., Kakatu, A., & Mukoh, A. (1993). *J. Appl. Phy.*, *73*, 4743.
[4] Centore, R., & Garzillo, C. (1997). *J. Chem. Soc., Perkin Trans.*, *2*, 79.
[5] Centore, R., Panunzi, B., Roviello, A., Sirigu, A., & Villano, P. (1996). *Mol. Cryst. Liq. Cryst.*, *275*, 107.
[6] Madhusudana, N. V., Shashidhar, R., & Chandrasekhar, S. (1971). *Mol. Cryst. Liq. Cryst.*, *13*, 61.
[7] Pelzl, G. (2000). Symmetry and Chirality in Liquid Crystals. In: *Handbook of Liquid Crystals*, Demus, D., Goodby, J., Garg, G. W., Spicess, H.-W., & Vill, V. (Eds.), Wiley: Weinheim, Vol. 2, 128.
[8] Wilfrid, G. S., & Glenn, H. B. (1959). *J. Am. Chem. Soc.*, *81*, 2532.
[9] Artigas, M., Marcos, M., Melendez, E., & Serrano, J. L. (1985). *Mol. Cryst. Liq. Cryst.*, *130*, 337.
[10] Barbera, J., Marcos, M., & Serrano, J. L. (1987). *Mol. Cryst. Liq. Cryst.*, *149*, 225.
[11] Bennur, S. C., Gault, J. D., Krion, T., & Ourigues, G. R. (1986). *Mol. Cryst. Liq. Cryst.*, *154*, 267.
[12] Kodaka, M., Shah, S. N., Tomohiro, T., & Chudgar, N. K. (1998). *J. Phys. Chem. B.*, *102*, 1219.
[13] Van Deun, R., Parac-Vogt, T. N., Van Hecke, K., Van Meervelt, L., Binnemans, K., Guillon, D., & Donnio, B. (2003). *J. Mater. Chem.*, *13*, 1639.
[14] Sandhya, Y. K., Pillai, C. K. S., & Kumar, K. S. (2004). *J. Polym. Sci. Polym. Phys.*, *42*, 1289.
[15] Chudgar, N. K., Sharma, H. C., & Shah, A. M. (1996). *Mol. Cryst. Liq. Cryst. Sci, Technol. C.*, *6*, 1.
[16] Yang, H., Wang, L., Cao, H., Shi, L., Wei, Q., & Wang, Y. (2008). *Liq. Cryst.*, *35*, 581.
[17] Kelker, H., & Scheurle, B. (1969). *Angew. Chem. Int. Ed. Engl.*, *81*, 903.
[18] Matsunaga, Y., Hikosaka, L., Hosono, K., Keda, N. Takahashi, T., & Uemura, Y. (2001). *Mol. Cryst. Liq. Cryst. Sci. Technol. Sect. A.*, *369*, 103.

[19] Yeap, G. Y., Ha, S. T., Lim, P. L., Boey, P. L., Ito, M. M., Sanehisa, S., & Youhei, Y. (2006). *Liq. Cryst.*, *33*, 205.
[20] Campillos, E., Marcos, M., Oriol, L. T., & Serrano, J. L. (1992). *Mol. Cryst. Liq. Cryst. Sci. Technol. Sect. A*, *215*, 127.
[21] Hu, P., Zhao, K. Q., Zhang, L. F., Lin, R., & Xu, H. B. (1999). *Acta Chim. Sin.*, *57*, 931.
[22] Shin, S. T., Choi, H., Lee, C. K., Kwon, S. S., Kim, T. S., Choi, E. J., Kim, S. Y., Zim, W. C., Kim, D. C., & Chien, L. C. (2004). *Liq. Cryst.*, *31*, 935.
[23] Umadevi, S., & Sadashiva, B. K. (2005). *Liq. Cryst.*, *32*, 1233.
[24] Centore, R., & Garzillo, C. (1997). *J. Chem. Soc., Perkin Trans.*, *2*, 79.
[25] Cajar, H. (1898). *Ber. deut. Chem. Ges.*, *31*, 2807.
[26] Kovganko, V. N., & Kovganko, N. N. (2006). *Russ. J. Org. Chem.*, *42*, 907.
[27] Singh, B., & Pandey, A. (2010). *Liq. Cryst.*, *37*, 57.